

AD A132 229

ADAPTIVE ARRAY BEHAVIOR WITH PERIODIC PHASE MODULATED  
INTERFERENCE(U) OHIO STATE UNIV COLUMBUS ELECTROSCIENCE  
LAB A S AL-RUWAIS ET AL. JUL 83 ESL-714505-3

1/1

UNCLASSIFIED

N00019-82-C-0190

F/G 9/5

NL

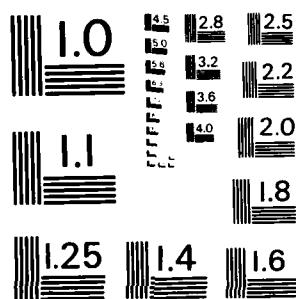
END

DATE

FORMED

10 83

BT



MICROCOPY RESOLUTION TEST CHART  
NATIONAL BUREAU OF STANDARDS - 1963 - A

8

OSU

The Ohio State University

ADAPTIVE ARRAY BEHAVIOR WITH PERIODIC PHASE  
MODULATED INTERFERENCE

A.S. Al-Ruwais  
R.T. Compton, Jr.

ADA 132229

The Ohio State University

**ElectroScience Laboratory**

Department of Electrical Engineering  
Columbus, Ohio 43212

Technical Report 714505-3

Contract No. N00019-82-C-0190

July 1983

APPROVED FOR PUBLIC RELEASE  
DISTRIBUTION UNLIMITED

Department of the Navy  
Naval Air Systems Command  
Washington, D.C. 20361

DTIC  
ELECTE  
SEP 08 1983  
S D E

DTIC FILE COPY

88 09 06 030

## NOTICES

When Government drawings, specifications, or other data are used for any purpose other than in connection with a definitely related Government procurement operation, the United States Government thereby incurs no responsibility nor any obligation whatsoever, and the fact that the Government may have formulated, furnished, or in any way supplied the said drawings, specifications, or other data, is not to be regarded by implication or otherwise as in any manner licensing the holder or any other person or corporation, or conveying any rights or permission to manufacture, use, or sell any patented invention that may in any way be related thereto.

REPORT DOCUMENTATION PAGE		1. REPORT NO. AD-A132229	2.	3. Recipient's Accession No.
4. Title and Subtitle ADAPTIVE ARRAY BEHAVIOR WITH PERIODIC PHASE MODULATED INTERFERENCE		5. Report Date July 1983		6.
7. Author(s) A.S. Al-Ruwais and R.T. Compton, Jr.		8. Performing Organization Rept. No. ESL 714505-3		9.
9. Performing Organization Name and Address The Ohio State University ElectroScience Laboratory Department of Electrical Engineering Columbus, Ohio 43212		10. Project/Task/Work Unit No.		11. Contract(C) or Grant(G) No. (C) (G) N00019-82-C-0190
12. Sponsoring Organization Name and Address Department of the Navy Naval Air Systems Command Washington, D.C. 20361		13. Type of Report & Period Covered Technical Report		14.
15. Supplementary Notes				
16. Abstract (Limit: 200 words) <p>This report discusses the behavior of an LMS adaptive array <sup>C</sup> when receiving a phase modulated interference signal. A mathematical technique is presented for computing the time behavior of the array weights with such interference. This technique is then used to study the behavior of a 2-element array receiving an interference signal with sinusoidal phase modulation. The effects of the interference phase modulation on desired signal modulation, output SINR (signal-to-interference-plus-noise ratio) and desired signal bit error probability are discussed.</p>				
17. Document Analysis a. Descriptors				
Adaptive Arrays Interference Rejection		Phase Modulation Antijam		
b. Identifiers/Open-Ended Terms				
c. COSATI Field/Group				
18. Availability Statement APPROVED FOR PUBLIC RELEASE DISTRIBUTION <u>UNLIMITED</u>		19. Security Class (This Report) Unclassified		21. No. of Pages 41
		20. Security Class (This Page) Unclassified		22. Price

# TABLE OF CONTENTS

	PAGE
LIST OF FIGURES	111
I. INTRODUCTION	1
II. FORMULATION OF THE PROBLEM	2
III. AN EXAMPLE	17
A. Typical Waveforms	21
B. The Effect of Angle of Arrival	26
C. The Effect of Modulation Index and Frequency	29
D. The Effect of Interference-To-Noise Ratio	29
E. The Effect of Desired Signal-To-Noise Ratio	34
F. Bit Error Probability	34
IV. CONCLUSIONS	37
REFERENCES	41

Accession For		
NTIS	DTIC	<input checked="" type="checkbox"/>
DTIC	USCIB	<input type="checkbox"/>
USCIB	Other	
By		
Date		
Approved by		
Special		
Dist		
<b>A</b>		



# LIST OF FIGURES

FIGURE		PAGE
1	The LMS Adaptive Array.	4
2	$a_{dn}(t')$ versus time.	22
3	Output INR versus time.	24
4	SINR versus time.	25
5	$m$ versus $\theta_i$ .	27
6	$a_{max}$ versus $\theta_i$ .	28
7	$a_{max}$ versus $f_m'$ .	30
8	$m$ versus $f_m'$ .	31
9	$a_{max}$ versus $f_m'$ .	32
10	$m$ versus $f_m'$ .	33
11	$m$ versus $f_m'$ .	35
12	$a_{max}$ versus $f_m'$ .	36
13	Bit error probability versus $f_m'$ .	38
14	Bit error probability versus $f_m'$ .	39

## I. INTRODUCTION

The performance of an LMS (least mean square) adaptive array [1] can be influenced by the modulation on an interference signal. For example, pulsed interference can make the weights in the array alternate back and forth between two sets of values, one when the interference is on and the other when it is off [2]. Interference modulation has two deleterious effects on the array. First, it can make the array modulate the desired signal. Second, it can cause the array output SINR (signal-to-interference-plus-noise ratio) to vary with time. In a digital communications system, such SINR variation usually results in an increased bit error probability. For these effects to occur, the modulation parameters must be properly chosen. For example, the modulation rate must be commensurate with the array speed of response.

In previous studies, the authors have examined the effects on an adaptive array of interference with pulsed modulation [2], with sinusoidal, suppressed carrier envelope modulation [3] and with arbitrary periodic envelope modulation [4]. Each of these studies involved interference with envelope modulation but not phase modulation.

The purpose of the present report is to extend the earlier work to handle interference with phase modulation. We assume an adaptive array receives an interference signal with a periodic but otherwise arbitrary phase modulation. We present a method of solving for the resulting time-varying array weights. Using this method, we then study as an



example the behavior of a 2-element array that receives an interference signal with sinusoidal phase modulation. We show how each interference signal parameter affects the desired signal modulation, the SINR variation and the bit error probability.

In Section II, we formulate the problem and present the mathematical technique for solving for the array weights. In Section III, we describe the 2-element array and the phase modulated interference signal and present our numerical results. Section IV contains the conclusions.

## II. FORMULATION OF THE PROBLEM

Assume an adaptive array consists of  $J$  isotropic elements with half wavelength spacing, as shown in Figure 1. Let  $\tilde{x}_j(t)$  be the analytic signal received on element  $j$ .  $\tilde{x}_j(t)$  is multiplied by a complex weight  $w_j$  and then summed to produce the array output  $\tilde{s}(t)$ . The array weights are controlled by LMS (least mean square) feedback loops [1], which obtain each weight  $w_j$  by integrating the product of  $\tilde{x}_j(t)$  with the error signal  $\tilde{\varepsilon}(t)$ . The error signal is the difference between the reference signal  $\tilde{r}(t)$  and the array output  $\tilde{s}(t)$ . The array weights satisfy the differential equation

$$\frac{dW}{dt} + k\Phi W = kS, \quad (1)$$

where  $W = [w_1, w_2, \dots, w_J]^T$  is the weight vector,  $t$  is time,  $\Phi$  is the covariance matrix,

$$\Phi = E(X^* X^T) \quad , \quad (2)$$

S is the reference correlation vector,

$$S = E[X^* \tilde{r}(t)] \quad , \quad (3)$$

and k is the LMS loop gain. In these equations, X is the signal vector,

$$X = [\tilde{x}_1(t), \tilde{x}_2(t), \dots, \tilde{x}_J(t)]^T \quad , \quad (4)$$

T denotes transpose, \* complex conjugate and E(.) expectation.

We assume that a desired signal and an interference signal are incident on the array and that thermal noise is present in each element signal. The signal vector then contains three terms,

$$X = X_d + X_i + X_n \quad , \quad (5)$$

where  $X_d$ ,  $X_i$ , and  $X_n$  are the desired, interference and noise vectors, respectively.

Let the desired signal be a CW (single frequency) signal incident from angle  $\theta_d$  relative to broadside. ( $\theta$  is defined in Figure 1.) The desired signal vector is then

$$X_d = A_d e^{j(\omega_0 t + \psi_d)} U_d \quad , \quad (6)$$

where  $A_d$  is the amplitude,  $\omega_0$  is the carrier frequency,  $\psi_d$  is the carrier phase angle, and  $U_d$  is a vector containing the interelement phase shifts,

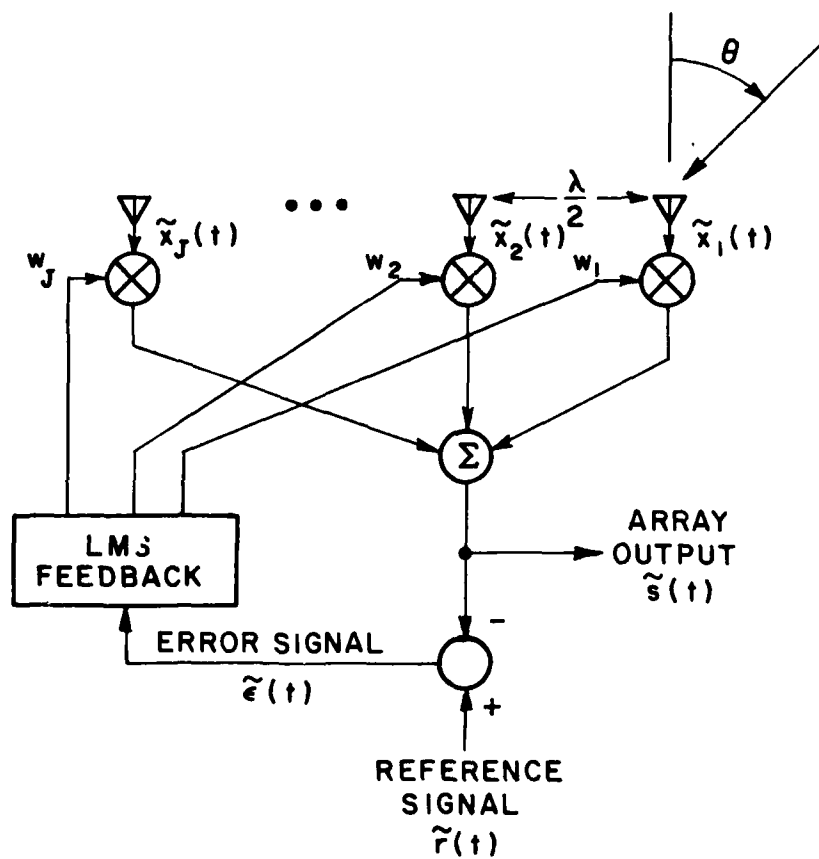


Figure 1. The LMS Adaptive Array.

$$U_d = [1, e^{-j\phi_d}, \dots, e^{-jK\phi_d}]^T, \quad (7)$$

where

$$\phi_d = \pi \sin \theta_d, \quad (8)$$

and where, to simplify notation, we let

$$K = J - 1. \quad (9)$$

We assume  $\psi_d$  is a random variable uniformly distributed on  $(0, 2\pi)$ .

Next, assume an angle modulated interference signal arrives from angle  $\theta_i$ . The interference signal vector is

$$X_i = A_i e^{j(\omega_0 t + \psi_i)} U_i(t), \quad (10)$$

with

$$U_i(t) = \begin{pmatrix} e^{j\gamma_i(t)} \\ e^{j[\gamma_i(t-T_i)-\phi_i]} \\ e^{j[\gamma_i(t-2T_i)-2\phi_i]} \\ \vdots \\ e^{j[\gamma_i(t-KT_i)-K\phi_i]} \end{pmatrix}, \quad (11)$$

where  $\gamma_i(t)$  is the angle modulation as received on element 1,  $A_i$  is the interference amplitude and  $\psi_i$  is the carrier phase angle.  $T_i$  and  $\phi_i$  are the interelement time delay and carrier phase shift,

$$T_i = \frac{\pi}{\omega_0} \sin \theta_i, \quad (12)$$

and

$$\phi_i = \omega_0 T_i = \pi \sin \theta_i. \quad (13)$$

We assume  $\psi_i$  is a random variable, uniformly distributed on  $(0, 2\pi)$  and statistically independent of  $\psi_d$ .

Finally, we assume each element signal contains a zero-mean, independent Gaussian thermal voltage  $\tilde{n}_j(t)$  of power  $\sigma^2$ . The noise vector is

$$\chi_n = [\tilde{n}_1(t), \tilde{n}_2(t), \dots, \tilde{n}_J(t)]^T, \quad (14)$$

where

$$E[\tilde{n}_j^*(t) \tilde{n}_k(t)] = \sigma^2 \delta_{jk}, \quad 1 \leq j, k \leq J, \quad (15)$$

with  $\delta_{jk}$  the Kronecker delta. The  $\tilde{n}_j(t)$  are assumed statistically independent of both  $\psi_d$  and  $\psi_i$ .

Under these assumptions, the covariance matrix in (2) is the sum of a desired, an interference and a noise term,

$$\Phi = \Phi_d + \Phi_i + \Phi_n. \quad (16)$$

The desired signal term is

$$\Phi_d = E(X_d^* X_d^T) = A_d^2 U_d^* U_d^T \quad (17)$$

The interference term is

$$\Phi_i = E(X_i^* X_i^T) = A_i^2 \begin{bmatrix} 1 & e^{j[x_{01}(t) - \phi_i]} & \dots & e^{j[x_{0K}(t) - K\phi_i]} \\ e^{j[x_{10}(t) + \phi_i]} & 1 & \dots & e^{j[x_{1K}(t) - (K-1)\phi_i]} \\ \cdot & \cdot & & \cdot \\ \cdot & \cdot & & \cdot \\ \cdot & \cdot & & \cdot \\ \cdot & \cdot & & \cdot \\ e^{j[x_{K0}(t) + K\phi_i]} & e^{j[x_{K1}(t) + (K-1)\phi_i]} & \dots & 1 \end{bmatrix} \quad (18)$$

where

$$x_{pq}(t) = \gamma_i(t - qT_i) - \gamma_i(t - pT_i) \quad (19)$$

and where p and q are integers between 0 and K. The noise term is

$$\Phi_n = \sigma^2 I \quad (20)$$

with I the identity matrix.

To compute the reference correlation vector  $S$  in (3), we must specify the reference signal  $\tilde{r}(t)$ . In practical applications, the reference signal is derived from the array output [5,6,7]. To make the array perform properly, it must be a signal correlated with the desired signal and uncorrelated with the interference. Here we assume the reference signal to be a replica of the desired signal,

$$\tilde{r}(t) = A_r e^{j(\omega_0 t + \psi_d)} \quad , \quad (21)$$

where  $A_r$  is its amplitude. Equation (3) then yields

$$S = A_r A_d^* U_d^* \quad . \quad (22)$$

When (16) and (22) are substituted into (1), we find that the weights satisfy a system of differential equations with constants on the right but with time-varying coefficients (due to  $\phi_i$ ). In the rest of this section, we develop a method for solving this system of equations.

To solve (1), we do several things. First, we write the interference covariance matrix in a more compact form. We define  $J$  vectors,

$$\begin{aligned} V_0 &= (1, 0, 0 \dots 0, 0)^T \quad , \\ V_1 &= (0, e^{-j\phi_i}, 0, \dots 0, 0)^T \quad , \\ V_2 &= (0, 0, e^{-j2\phi_i}, \dots, 0, 0)^T \quad , \\ &\vdots \\ &\vdots \end{aligned}$$

and

$$V_K = (0, 0, 0 \dots 0, e^{-jK\phi_i})^T \quad (23)$$

Note that these  $J$  vectors form an orthonormal set,

$$V_j^T V_k^* = \delta_{jk}, \quad 0 < j, k < K \quad (24)$$

By using these vectors,  $\phi_i$  in (18) may be written

$$\phi_i = A_i^2 \sum_{p=0}^K \sum_{q=0}^K e^{jx_{pq}(t)} V_p^* V_q^T, \quad (25)$$

so (1) becomes

$$\frac{dW}{dt} + k [A_d^2 U_d^* U_d^T + A_i^2 \sum_{p=0}^K \sum_{q=0}^K e^{jx_{pq}(t)} V_p^* V_q^T + \sigma^2 I] W = k A_r A_d U_d^* \quad (26)$$

Next, we normalize (26). Dividing by  $k\sigma^2$  gives

$$\frac{dW(t')}{dt'} + [\phi_2 + \epsilon_i \sum_{p=0}^K \sum_{q=0}^K e^{jx_{pq}(t')} V_p^* V_q^T] W(t') = \frac{A_r}{\sigma} \sqrt{\epsilon_d} U_d^*, \quad (27)$$

where

$$\phi_2 = I + \epsilon_d U_d^* U_d^T, \quad (28)$$



$$\xi_d = \frac{A_d^2}{\sigma^2} = \text{input signal-to-noise ratio (SNR) per element,}$$

$$\xi_i = \frac{A_i^2}{\sigma^2} = \text{input interference-to-noise ratio (INR) per element,}$$

and where

$$t' = k\sigma^2 t = \text{normalized time .} \quad (29)$$

Also, we note that the constant  $\frac{A_r}{\sigma}$  on the right will just appear as a scale factor in the solution for  $W(t')$ . It has no effect on the array output SINR to be discussed below. Hence we arbitrarily set  $\frac{A_r}{\sigma} = 1$  to eliminate it. Equation (27) is then

$$\frac{dW(t')}{dt'} + [\phi_2 + \xi_i \sum_{p=0}^K \sum_{q=0}^K e^{jx_{pq}(t')} v_p^* v_q^T] W(t') = \sqrt{\xi_d} U_d^* . \quad (30)$$

Next, in order to be able to solve (30), we make the important assumption that the angle modulation  $\gamma_i(t)$  is periodic. If  $\gamma_i(t)$  is periodic, the functions  $e^{jx_{pq}(t')}$  are also periodic. Therefore we may expand each of them in a Fourier series. In order to simplify notation later, we shall also include the constant  $\xi_i$  in this expansion. Thus, we write

$$\xi_i e^{jx_{pq}(t')} = \sum_{\ell=-\infty}^{\infty} f_{\ell pq} e^{j\ell\omega_m' t'} , \quad (31)$$

where  $f_{\ell pq}$  is the  $\ell$ th Fourier coefficient of  $\xi_i e^{j x_{pq}(t')}$  and  $\omega'_m$  is the normalized fundamental frequency of  $\gamma_i(t')$ , i.e.,

$$\omega'_m = \omega_m / k \sigma^2 \quad , \quad (32)$$

where  $\omega_m$  is the fundamental frequency of  $\gamma_i(t)$ . We note for later use that if  $p=q$ , then  $x_{pq}(t') = 0$ , so the series in (31) contains only a zero frequency term, i.e.,

$$f_{\ell pp} = \xi_i \delta_{\ell 0} \quad . \quad (33)$$

Also, it is easily shown that

$$f_{\ell qp} = f_{-\ell pq}^* \quad , \quad (34)$$

and

$$f_{\ell(p+1)(q+1)} = f_{\ell pq} e^{-j \ell \omega'_m T_i} \quad . \quad (35)$$

In addition to assuming  $\gamma_i(t)$  periodic, we shall also assume that the bandwidth of the interference is finite, i.e., we assume that only a finite number of terms are nonzero in (31). Suppose the coefficients in (31) are zero for  $|\ell| > L$ , where  $L$  is some integer.

Then

$$\xi_i e^{j x_{pq}(t')} = \sum_{\ell=-L}^L f_{\ell pq} e^{j n \omega'_m t'} \quad . \quad (36)$$

Since (30) is a linear differential equation with periodic coefficients, the solution for  $W(t')$  will be a periodic function of time after any initial transients have died out [8]. In this paper, we shall not attempt to solve for initial transients, but shall consider only the periodic steady-state solution. Once any initial transients are over,  $W(t')$  can be written as a Fourier series,

$$W(t') = \sum_{n=-\infty}^{\infty} C_n e^{jn\omega_m' t'} \quad (37)$$

where  $C_n$  is a vector Fourier coefficient. Substituting this series into (30) and enforcing the resulting equation for each frequency component separately gives

$$(\phi_2 + jn\omega_m' I)C_n + \sum_{\ell=-L}^L \sum_{p=0}^K \sum_{q=0}^K f_{\ell pq} V_p^* V_q^T C_{n-\ell} = \sqrt{\epsilon_d} U_d^* \delta_{no}, \quad -\infty < n < \infty. \quad (38)$$

Equation (38) is an infinite system of vector equations, one for each  $n$ . To solve for the  $C_n$ , we first assume that there is some integer  $N$  such that the Fourier coefficients  $C_n$  are negligible for  $|n| > N$ . In other words, we assume  $W(t')$  can be adequately approximated by a finite sum

$$W(t') = \sum_{n=-N}^N C_n e^{jn\omega_m' t'} \quad (39)$$

Such an approximation is reasonable because the feedback loops controlling the array weights in  $W(t')$  are lowpass filter loops that cannot respond above a certain speed.

If we set  $C_n=0$  for  $|n| > N$ , then (38) yields a finite system of equations for the remaining  $C_n$ . Each vector  $C_n$  has  $J$  scalar components, so the result is a system of  $(2N+1)J$  linear equations in the unknown scalar components. One could solve for  $W(t')$  by solving this system of equations numerically.

However, rather than work with (38) directly, we shall instead transform variables first. We do this because the resulting equations have a more systematic form. Specifically, we shall express each  $C_n$  in terms of its components along the vectors  $V_k$  in (23). (Since each  $C_n$  has  $J$  components, the  $J$  orthonormal vectors  $V_k$  can serve as basis vectors.) We write

$$C_n = \sum_{k=0}^K \alpha_{n,k} V_k^* \quad , \quad (40)$$

where the  $\alpha_{n,k}$  are scalar coefficients.  $\alpha_{n,k}$  is the component of  $C_n$  along the unit vector  $V_k^*$ . Substituting (40) into (38), multiplying the result on the left by  $V_a^T$  (for  $a=0,1,2, \dots, K$ ) and using (24) yields the equation

$$jn\omega_m' \alpha_{n,a} + \sum_{k=0}^K Q_{ak} \alpha_{n,k} + \sum_{\ell=-L}^L \sum_{q=0}^K f_{\ell a q} \alpha_{n-\ell,q} = \sqrt{\epsilon_d} (V_a^T U_d^*) \delta_{no} \quad , \quad (41)$$

where

$$Q_{ak} = V_a^T \Phi_2 V_k^* \quad . \quad (42)$$

In (41), we have  $0 < a < K$  and it is understood that  $\alpha_{m,q} = 0$  whenever  $|m| > N$ .  $Q_{ak}$  is readily found from (23) and (28):

$$Q_{ak} = \delta_{ak} + \epsilon_d e^{j(a-k)(\phi_d - \phi_i)} . \quad (43)$$

Also, we find from (7) and (23) that

$$V_a^T U_d^* = e^{ja(\phi_d - \phi_i)} , \quad 0 < a < K . \quad (44)$$

Equation (41), when written out, yields a finite system of equations of the form

$$MA = B , \quad (45)$$

where  $A$  is a vector containing the unknown coefficients  $\alpha_{n,k}$  ,

$$A = (\alpha_{N,0}, \alpha_{N,1}, \dots, \alpha_{N,K}, \alpha_{N-1,1}, \dots, \alpha_{N-1,K}, \dots, \alpha_{-N,1}, \dots, \alpha_{-N,K})^T , \quad (46)$$

$B$  is a vector obtained from the right hand side of (41), and  $M$  is the matrix of coefficients obtained from the left side of (41). We give an example of  $M$  and  $B$  below in Section III. The numerical results presented below have been obtained by solving (41) numerically.

For this method to yield accurate results,  $N$  must be chosen large enough that at least  $2LJ$  of the  $\alpha_{n,k}$  are essentially zero on each end of the vector  $A$  in (46). If this vector has  $2LJ$  zeros on each end, the solution obtained from (41) will yield the same result as the solution

of the infinite system in (38). In practice, a suitable value of  $N$  may be determined by increasing  $N$  until the  $A$  vector has  $2LJ$  negligible terms on each end and until the values of the  $\alpha_{n,k}$  in the middle of the vector  $A$  are unaffected by further increases in  $N$ . Experience shows how large  $N$  must be in specific cases\*. Once the  $\alpha_{n,k}$  have been found, the  $C_n$  may be found from (40) and  $W(t')$  from (39).

The time-varying array weights have two effects on array performance. They cause the array to modulate the desired signal, and they cause the array output SINR to vary with time. In the remainder of this section, we discuss the calculation of these effects.

Given a time-varying weight vector  $W(t')$ , the desired signal component of the array output is

$$\tilde{s}_d(t') = A_d W^T(t') U_d e^{j(\omega'_0 t' + \psi_d)} , \quad (47)$$

where  $\omega'_0 = \omega_0 / k\sigma^2$ . To study the modulation on  $\tilde{s}_d(t)$ , we define

$$a_d(t') e^{jn_d(t')} = A_d W^T(t') U_d . \quad (48)$$

Then  $a_d(t') = A_d |W^T(t') U_d|$  is the envelope modulation and  $n_d(t') = \angle W^T(t') U_d$  is the phase modulation. Furthermore, we define  $a_{dn}(t')$  to be

\*The numerical solution of (41) was done using a Gauss elimination routine with full pivoting [9]. We have not examined the eigenvalue behavior of  $M$  in detail, but we did not experience any convergence problems or other unusual behavior due to ill-conditioning with this approach.

the envelope normalized to its value in the absence of interference,  
i.e.,

$$a_{dn}(t') = \frac{a_d(t')}{A_d |W_0^T U_d|} \quad , \quad (49)$$

where  $W_0$  is the steady-state weight vector that would occur without interference,

$$W_0 = (\Phi_d + \Phi_n)^{-1} S \quad . \quad (50)$$

( $\Phi_d$ ,  $\Phi_n$  and  $S$  are given in (17), (20) and (22).) Our results below are presented in terms of  $a_{dn}(t')$ , because the effect of the interference can be seen directly by comparing  $a_{dn}(t')$  with unity.

The output desired signal power is

$$P_d(t') = \frac{1}{2} E[|s_d(t')|^2] = \frac{1}{2} A_d^2 |W^T(t') U_d|^2 \quad . \quad (51)$$

The output interference power is

$$P_i(t') = \frac{1}{2} A_i^2 |W^T(t') U_i(t')|^2 \quad , \quad (52)$$

where  $U_i(t')$  is the vector of phasors given in (11) but written in terms of normalized time  $t' = \kappa \sigma^2 t$ . The output thermal noise power is

$$P_n(t') = \frac{\sigma^2}{2} W^T(t') W^*(t') \quad . \quad (53)$$

From these quantities, the output interference-to-noise ratio (INR),

$$\text{INR} = \frac{P_i(t')}{P_n(t')} , \quad (54)$$

and the output signal-to-interference-plus-noise ratio (SINR),

$$\text{SINR} = \frac{P_d(t')}{P_i(t') + P_n(t')} , \quad (55)$$

may be computed as functions of  $t'$ .

In the next section, we present an example using this technique and discuss the effects of a phase modulated interference signal on the adaptive array.

### III. AN EXAMPLE

Consider an array with two elements, so  $J=2$  and  $K=1$ . Let the interference have sinusoidal phase modulation,

$$\gamma_i(t') = \beta \sin \omega_m' t' , \quad (56)$$

where  $\beta$  is the maximum phase deviation (or the modulation index) and  $\omega_m'$  is the normalized modulation frequency. Then one finds from (19) and standard trigonometric identities that

$$e^{jX_{01}(t')} = e^{j\beta' \sin[\omega_m' (t' - \frac{T_1}{2}) - \frac{\pi}{2}]} , \quad (57)$$



where

$$\beta' = 2\beta \sin \frac{\omega_m' T_i'}{2}, \quad (58)$$

(and  $T_i' = k\sigma^2 T$ ). Using the Fourier Series expansion [10],

$$e^{jz \sin \rho} = \sum_{\ell=-\infty}^{\infty} J_{\ell}(z) e^{j\ell \rho}, \quad (59)$$

we find

$$\varepsilon_i e^{jx_{01}(t)} = \sum_{\ell=-\infty}^{\infty} f_{\ell 01} e^{j\ell \omega_m' t'}, \quad (60)$$

with

$$f_{\ell 01} = \varepsilon_i J_{\ell}(\beta') e^{-j\ell \left( \frac{\omega_m' T_i'}{2} + \frac{\pi}{2} \right)}. \quad (61)$$

From (34), we also have

$$f_{\ell 10} = f_{-\ell 01}^* = (-1)^{\ell} f_{\ell 01}, \quad (62)$$

since

$$J_{-\ell}(\beta') = (-1)^{\ell} J_{\ell}(\beta'). \quad (63)$$

To truncate the series in (60), we use the fact that

$$J_{\ell}(z) \approx 0 \text{ for } |\ell| > z + 1. \quad (64)$$

Thus, we approximate

$$\xi_i e^{j x_{01}(t')} = \sum_{\ell=-L}^L f_{\ell 01} e^{j \ell \omega_m' t'} \quad , \quad (65)$$

with

$$L = \{\beta' + 1\} = \{2\beta \sin \frac{\omega'_m T'_i}{2} + 1\} \quad , \quad (66)$$

where  $\{r\}$  denotes the smallest integer greater than  $r$ .

Writing out (41) with  $L=2$  as an example and with  $K=1$  gives the following matrix of coefficients  $M$  in (45):

[illegible]

The vectors A and S in (45) are

$$A = \begin{bmatrix} \alpha_{N,0} \\ \vdots \\ \vdots \\ \alpha_{2,0} \\ \vdots \\ \alpha_{0,1} \\ \alpha_{1,0} \\ \alpha_{1,1} \\ \alpha_{0,0} \\ \alpha_{0,1} \\ \alpha_{-1,0} \\ \alpha_{-1,1} \\ \vdots \\ \vdots \\ \vdots \\ \alpha_{-N,1} \end{bmatrix}, \quad S = \sqrt{\epsilon_d} \begin{bmatrix} 0 \\ \vdots \\ \vdots \\ \vdots \\ \vdots \\ 0 \\ 0 \\ 0 \\ 1 \\ e^{j(\phi_d - \phi_i)} \\ 0 \\ 0 \\ 0 \\ \vdots \\ \vdots \\ \vdots \\ 0 \end{bmatrix}, \quad (67)$$

where

$$F_\ell = \ell_{01}, \quad (68)$$

which, from (34), also implies

$$F_{-\ell}^* = f_{-\ell 01}^* = f_{\ell 10}, \quad (69)$$

and where

$$d_n = f_{000} + Q_{00} + jn\omega_m' = 1 + \epsilon_d + \epsilon_i + jn\omega_m', \quad (70)$$

and

$$Z = Q_{01} + f_{001} = \xi_d e^{j(\phi_i - \phi_d)} + \xi_i J_0(\beta') \quad (71)$$

To obtain the results presented below, we have solved this system (with the appropriate values of  $L$ ) numerically for the  $\alpha_{n,k}$ , and then evaluated  $C_n$  and  $W(t')$  from (40) and (39).

Let us now discuss the results obtained from these calculations. In part A below, we show typical curves of desired signal modulation, output INR and SINR as functions of time. In parts B-E, we describe the effect of each signal parameter on the desired signal modulation. In part F, we assume the array is used in a DPSK (differential phase shift keyed) digital communication system [11] and show how the bit error probability is affected by the interference signal parameters  $\xi_i$ ,  $\beta$  and  $f'_m$ .

#### A. Typical Waveforms

Figure 2 shows typical curves of the normalized envelope modulation  $a_{dn}(t')$  for  $\theta_d = 30^\circ$ ,  $\theta_i = 45^\circ$ ,  $\xi_d = 10$  dB,  $\xi_i = 30$  dB,  $f'_m = \frac{\omega'_m}{2\pi} = 10^2$ ,  $f'_0 = \frac{\omega'_0}{2\pi} = 10^8$ , and  $\beta = 10^2, 10^3, 10^4$  and  $10^5$ . These curves illustrate that the envelope modulation on the desired signal can be substantial for larger values of  $\beta$ .

It turns out that for this 2-element array, angle modulated interference does not cause phase modulation on the desired signal. This result was discovered by calculating  $\eta_d(t')$ , for numerous values

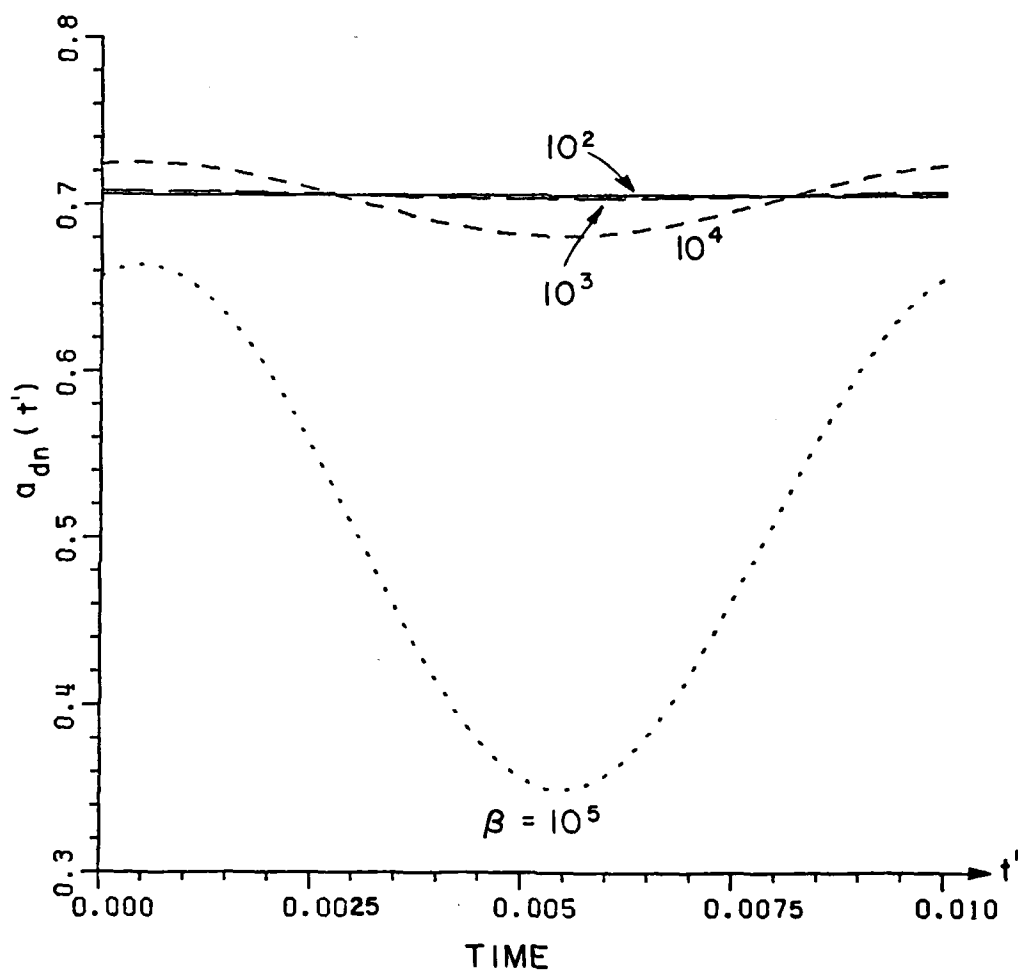


Figure 2.  $a_{dn}(t')$  versus time.

$\theta_d=30^\circ$ ,  $\theta_i=45^\circ$ ,  $\epsilon_d=10$  dB,  $\epsilon_i=30$  dB,

$f'_m=10^2$ ,  $f'_0=10^8$ .

of  $\theta_i$ ,  $\beta$ ,  $f'_m$  and  $\xi_i$ . These calculations show that  $\eta_d(t')$  does not change with time regardless of the signal parameters. The reason for this behavior is as follows. Both the amplitude and phase of each weight in the array vary sinusoidally with time. The amplitudes of the two weights are equal at each instant of time. The phase angle of each weight contains a term constant with time, which depends on interference arrival angle, and a term that varies sinusoidally with time. The sinusoidally varying term is  $180^\circ$  out of phase on the two weights. When a desired signal is passed through these weights the phase modulation produced on the desired signal by one weight is  $180^\circ$  out of phase with that produced by the other weight, and the sum signal at the array output contains no phase modulation.

Figures 3 and 4 show typical curves of the output INR and SINR as functions of time, over one period and for the same signal parameters as in Figure 2. Figure 3 shows that the average INR increases and the array SINR decreases as  $\beta$  increases. Also, as  $\beta$  increases, the INR and SINR variations with time are more pronounced. At low  $\beta$ , the INR and SINR are constant, because the array feedback tracks the incoming phase modulation.

In general one finds that the array behavior changes substantially as the signal parameters  $\theta_d$ ,  $\xi_d$ ,  $\theta_i$ ,  $\xi_i$ ,  $f'_m$  and  $\beta$  are varied. In parts B-E of this section, we examine the effect of each signal parameter on the desired signal modulation. In part F, we show how bit error probability is affected by the angle modulated interference when the array is used in a DPSK communication system.

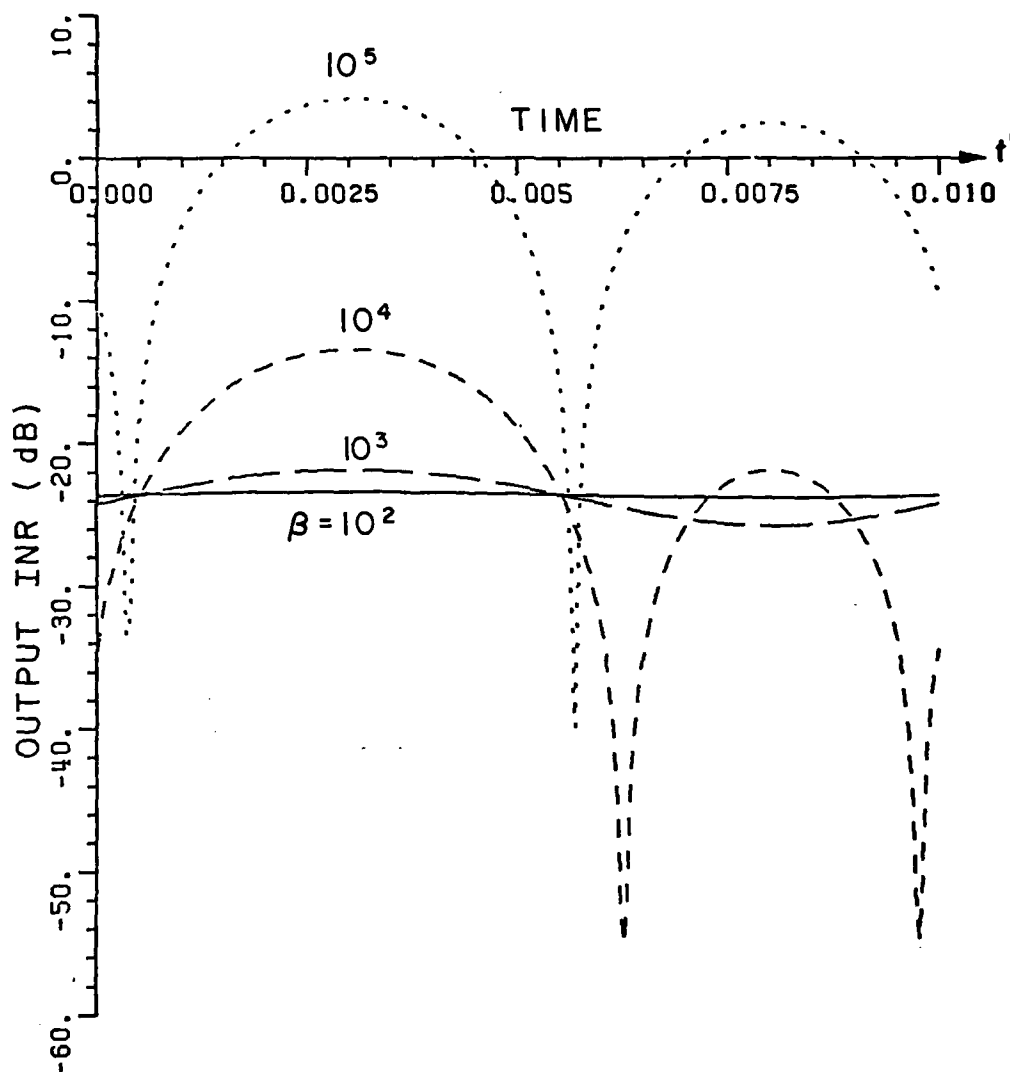


Figure 3. Output INR versus time.

$\theta_d=30^\circ$ ,  $\theta_i=45^\circ$ ,  $\xi_d=10$  dB,  $\xi_i=30$  dB,

$f'_m=10^2$ ,  $f'_o=10^8$ .

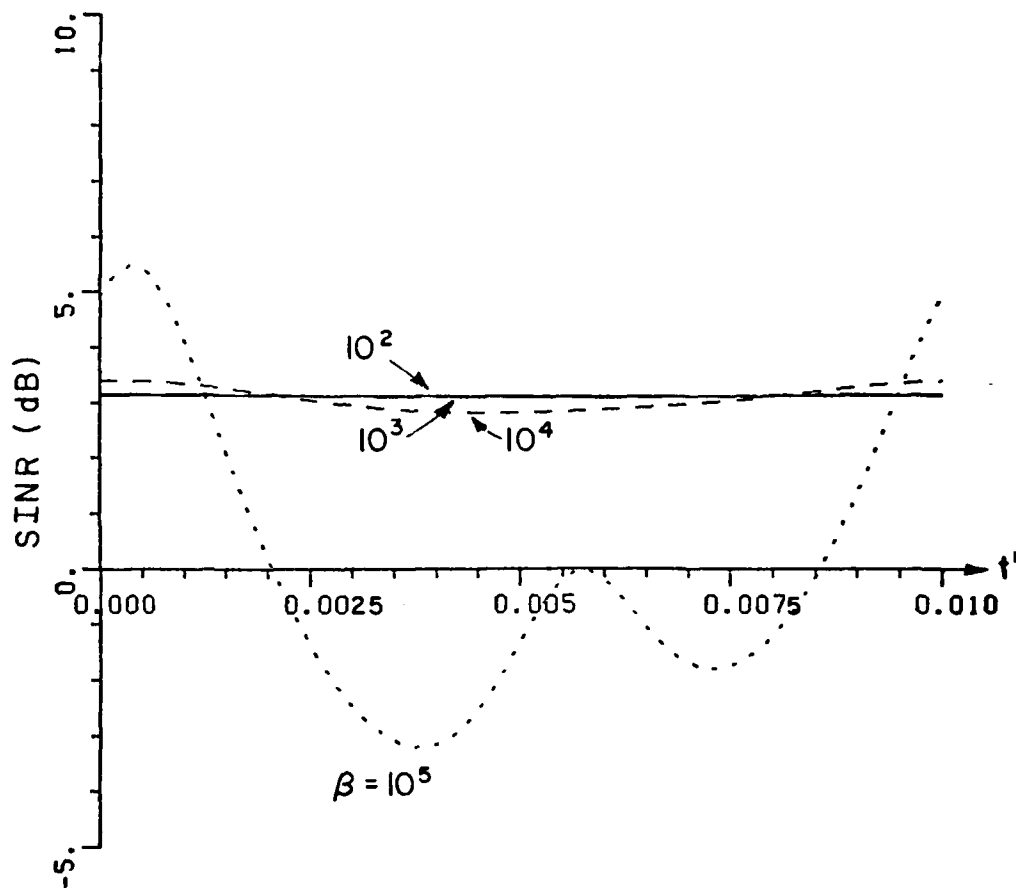


Figure 4. SINR versus time.

$\theta_d = 30^\circ$ ,  $\theta_i = 45^\circ$ ,  $\xi_d = 10$  dB,  $\xi_i = 30$  dB,

$f'_m = 10^2$ ,  $f'_o = 10^8$ .



To describe the desired signal modulation, we shall define three quantities. First, we let  $a_{\min}$  and  $a_{\max}$  be the minimum and maximum values of  $a_{dn}(t')$  during the modulation period. Then, we define

$$m = \frac{a_{\max} - a_{\min}}{a_{\max}} \quad . \quad (72)$$

$m$  is the envelope variation normalized to its peak. It may be thought of as "fractional modulation", analogous to percentage modulation in AM. In Parts B-E below, we describe the effect of each signal parameter on  $a_{\max}$  and  $m$ .

#### B. The Effect of Angle of Arrival

Desired signal modulation effects are small when  $\theta_i$  is far from  $\theta_d$ . When  $\theta_i$  is close to  $\theta_d$ , the envelope variation  $m$  is large and the peak  $a_{\max}$  is small. However, when  $\theta_i$  is equal to  $\theta_d$ , the desired signal is nulled, so  $m$  drops to a small value.

Figures 5 and 6 show typical curves of  $m$  and  $a_{\max}$  as functions of  $\theta_i$  for  $\theta_d=0^\circ$ ,  $\xi_d=10$  dB,  $\xi_i=40$  dB,  $f'_m=10^3$  and  $f'_o=10^8$ . Four different curves are shown, for  $\beta = 2 \times 10^3$ ,  $4 \times 10^3$ ,  $8 \times 10^3$  and  $10^4$ . It is seen that  $m$  is large and  $a_{\max}$  is small when  $\theta_i$  is near  $\theta_d$ . We note also that when  $\theta_i$  is extremely close to  $\theta_d$ ,  $m$  drops to zero. This behavior occurs because as  $\theta_i$  becomes very close to  $\theta_d$ , the peak-to-peak variation  $(a_{\max}-a_{\min})$  approaches zero more quickly than  $a_{\max}$  does, so  $m$  goes to zero. However, this behavior of  $m$  is of no importance, since the desired signal is nulled anyway.

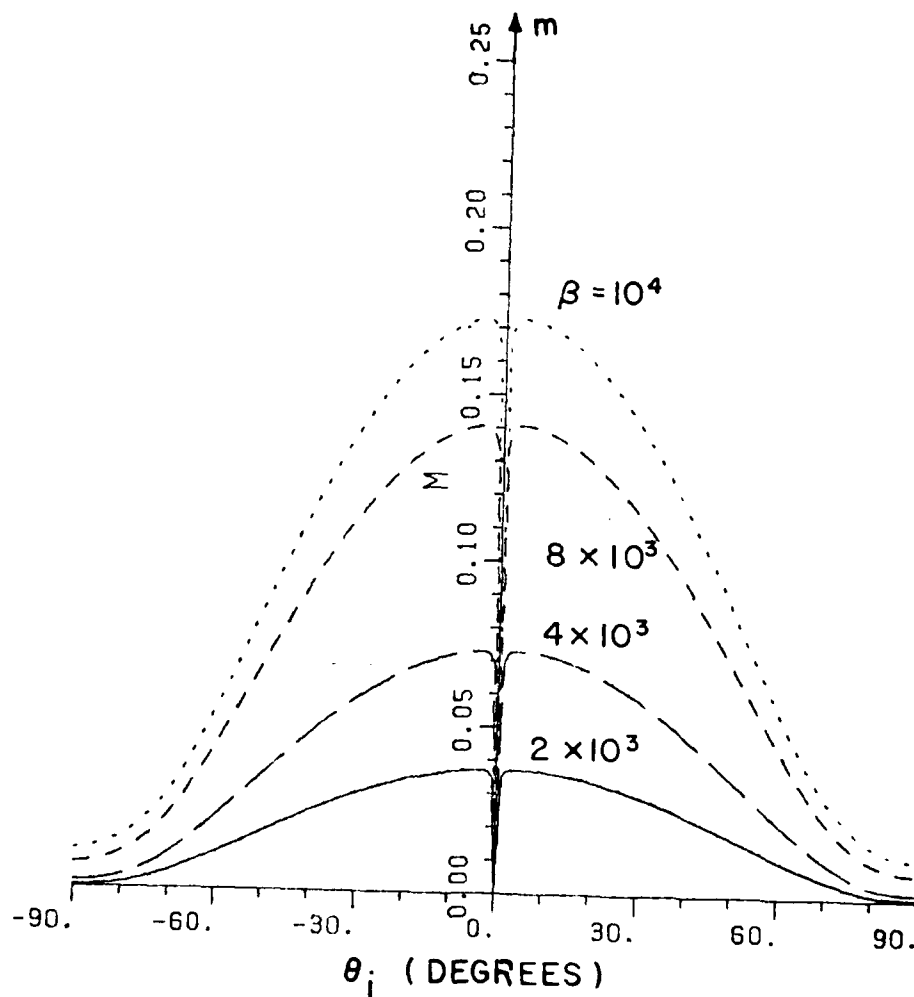


Figure 5.  $m$  versus  $\theta_i$ .

$\theta_d = 0^\circ$ ,  $\xi_d = 10$  dB,  $\xi_i = 40$  dB,

$f'_m = 10^3$ ,  $f'_o = 10^8$ .

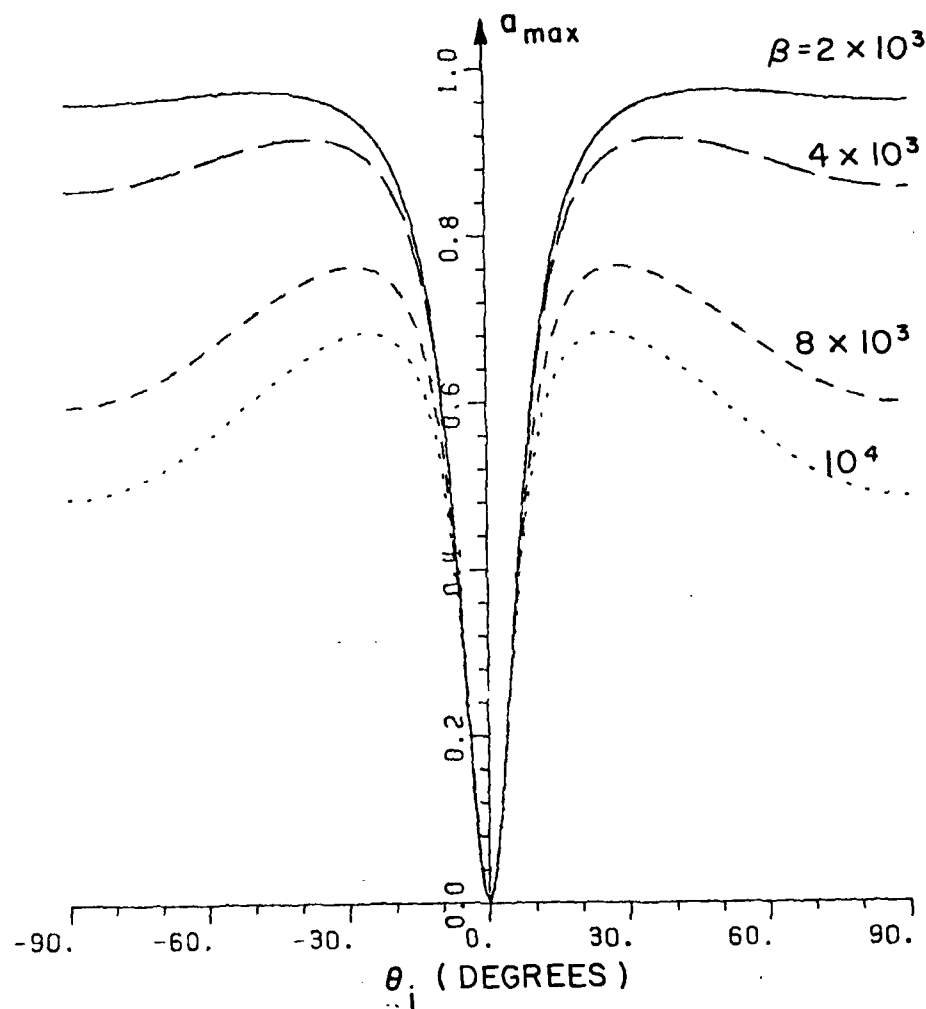


Figure 6.  $a_{\max}$  versus  $\theta_i$ .

$\theta_d = 0^\circ$ ,  $\epsilon_d = 10$  dB,  $\epsilon_i = 40$  dB,

$f'_m = 10^3$ ,  $f'_o = 10^8$ .

### C. The Effect of Modulation Index and Frequency

The peak  $a_{\max}$  is large at low  $f'_m$  and drops as  $f'_m$  increases. The higher  $\beta$ , the farther  $a_{\max}$  drops at high  $f'_m$ . The variation  $m$  is small at low  $f'_m$ , peaks at intermediate values of  $f'_m$  and drops as  $f'_m$  increases. For low and intermediate  $f'_m$ ,  $m$  is largest for high  $\beta$ . At high  $f'_m$ ,  $m$  drops more rapidly with larger values of  $\beta$ .

Figures 7 and 8 illustrate these results for the case  $\theta_d=30^\circ$ ,  $\theta_i=45^\circ$ ,  $\epsilon_d=10$  dB,  $\epsilon_i=30$  dB,  $f'_0=10^8$  and for values of  $\beta$  between  $2 \times 10^3$  and  $10^4$ . It is seen in Figure 7 that  $a_{\max}$  is large for low  $f'_m$  and drops as  $f'_m$  increases. This behavior is due to the array speed of response, which limits its ability to track the modulation at high  $f'_m$ .  $m$ , seen in Figure 8, peaks at intermediate  $f'_m$ .

### D. The Effect of Interference-To-Noise Ratio

For all values of  $f'_m$ , the variation  $m$  is largest for high INR.  $a_{\max}$  is high at low  $f'_m$  and drops at high  $f'_m$ .

Figures 9 and 10 show the behavior of  $a_{\max}$  and  $m$  versus  $f'_m$  for  $\theta_d=30^\circ$ ,  $\theta_i=45^\circ$ ,  $\epsilon_d=10$  dB,  $\beta=10^4$ ,  $f'_0=10^8$  and for four values of  $\epsilon_i$  between 20 and 45 dB. It may be seen in Figure 9 that  $a_{\max}$  peaks slightly at high INR, for values of  $f'_m$  around 400. This behavior is due to the change in array speed of response with INR.

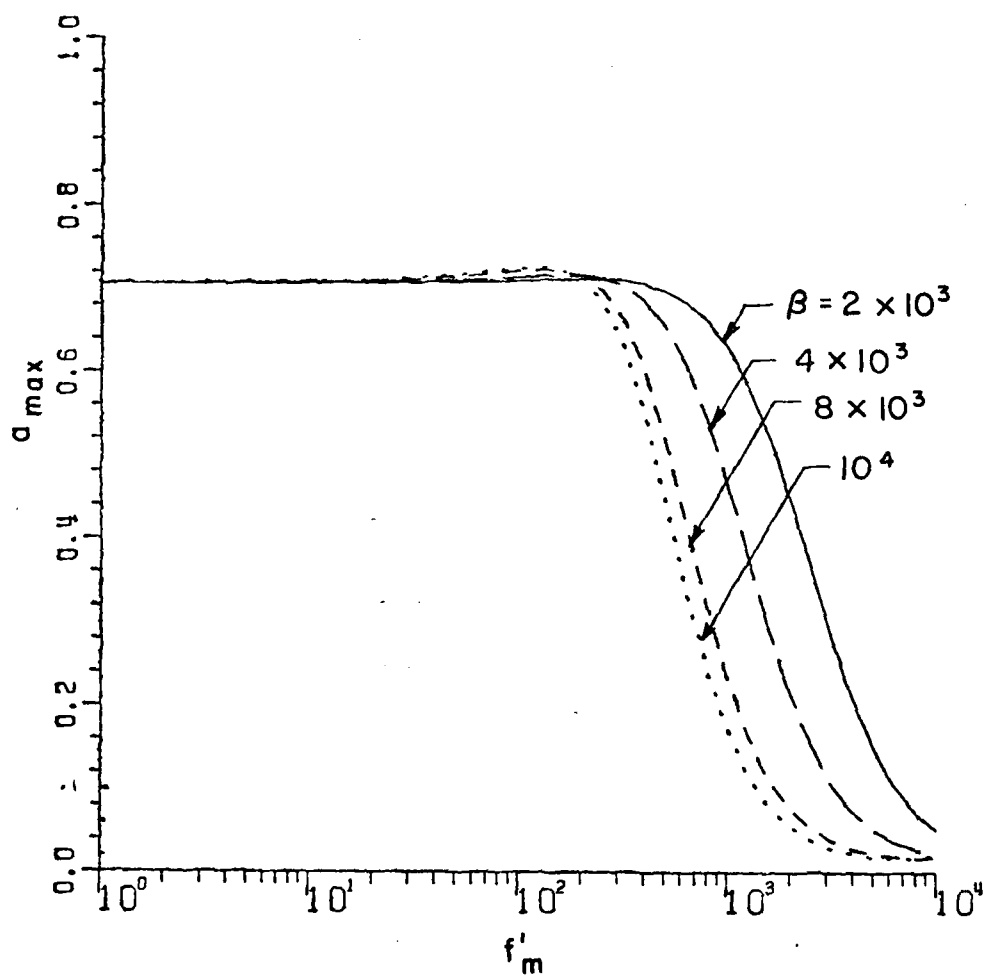


Figure 7.  $a_{\max}$  versus  $f'_m$ .

$\theta_d = 30^\circ$ ,  $\theta_i = 45^\circ$ ,  $\epsilon_d = 10$  dB,  $\epsilon_i = 30$  dB,

$f'_0 = 10^8$ .

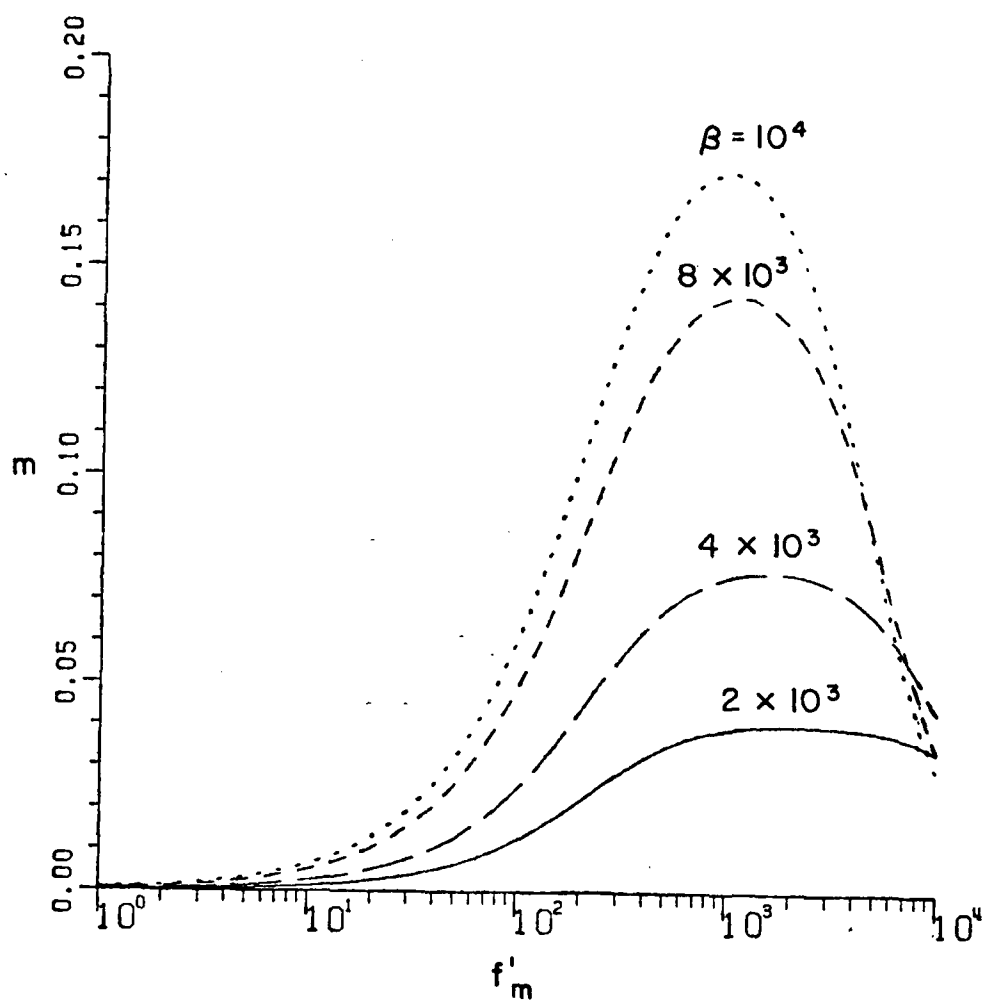


Figure 8.  $m$  versus  $f'_m$ .

$\theta_d = 30^\circ$ ,  $\theta_i = 45^\circ$ ,  $\xi_d = 10$  dB,  $\xi_i = 30$  dB,

$f'_0 = 10^8$ .

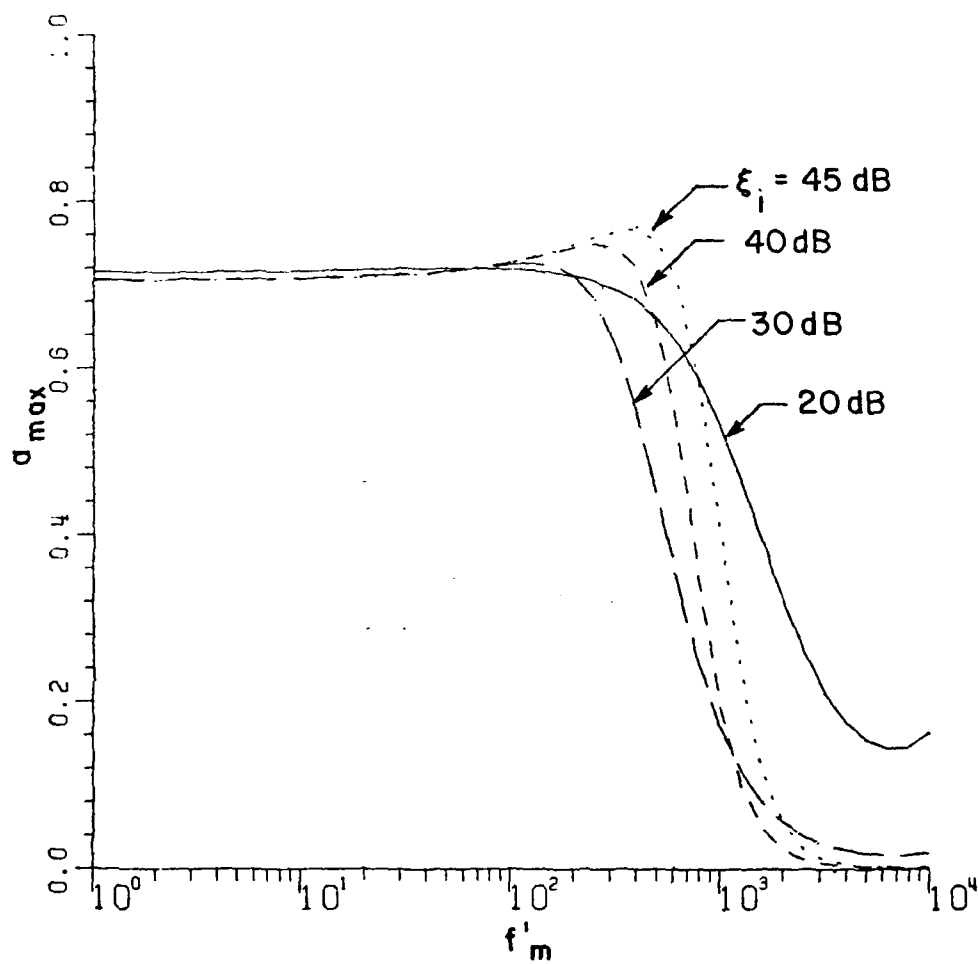


Figure 9.  $a_{\max}$  versus  $f'_m$ .

$\theta_d = 30^\circ$ ,  $\theta_i = 45^\circ$ ,  $\xi_d = 10$  dB,

$\beta = 10^4$ ,  $f'_0 = 10^8$ .

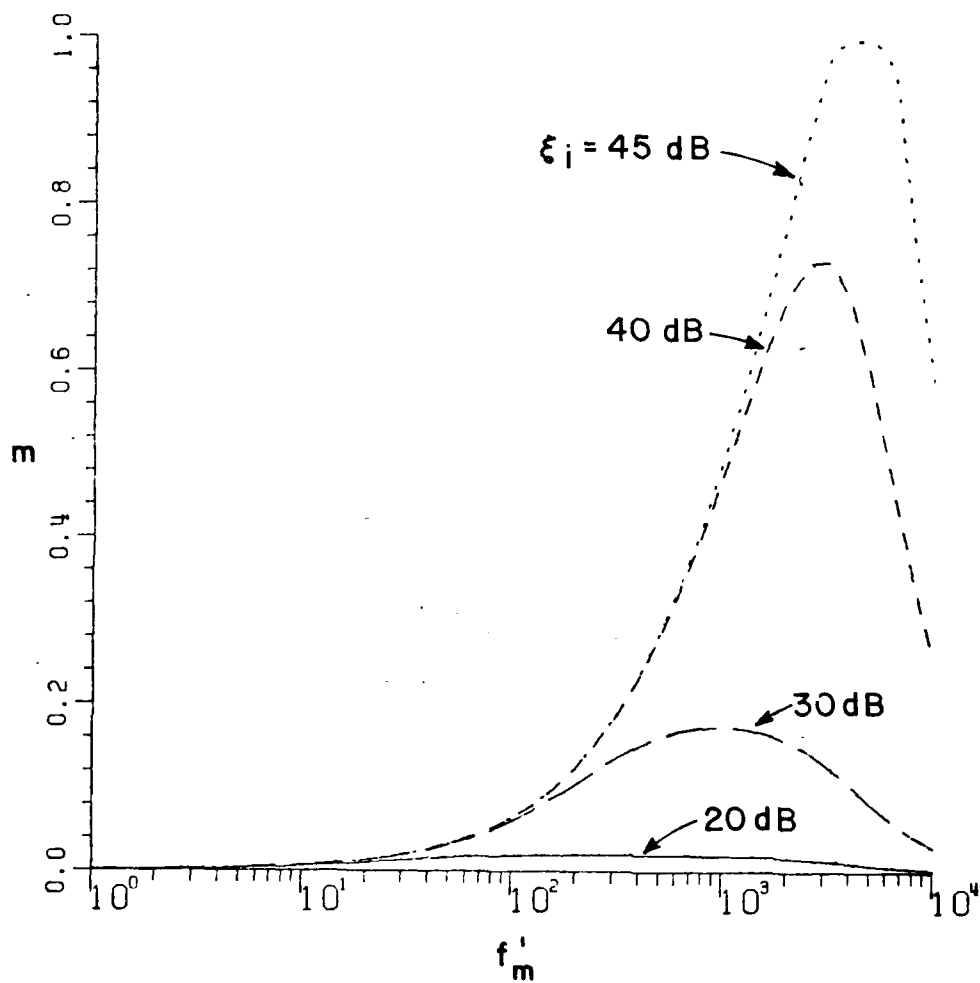


Figure 10.  $m$  versus  $f'_m$ .

$\theta_d = 30^\circ$ ,  $\theta_i = 45^\circ$ ,  $\epsilon_d = 10$  dB,

$\beta = 10^4$ ,  $f'_0 = 10^8$ .



#### E. The Effect of Desired Signal-To-Noise Ratio

$m$  is largest and  $a_{\max}$  is smallest for low  $\epsilon_d$ . As  $\epsilon_d$  is increased,  $m$  decreases and  $a_{\max}$  increases.

Figures 11 and 12 illustrate this behavior. Figure 11 shows  $m$  and Figure 12 shows  $a_{\max}$ , both versus  $f'_m$  for  $\theta_d=30^\circ$ ,  $\theta_i=45^\circ$ ,  $\epsilon_i=30$  dB,  $f'_0=10^8$ ,  $\beta=10^4$ , and for four values of  $\epsilon_d$  between 10 and 40 dB. It is seen that  $m$  peaks at intermediate  $f'_m$  with the value of  $f'_m$  at the peak dependent on  $\epsilon_d$ .

#### F. Bit Error Probability

To evaluate the effect of the time-varying SINR, we have computed the bit error probability when the desired signal is DPSK biphase modulated signal. We assume the desired signal bit duration is large compared with the propagation time across the array but small compared to the interference modulation period  $2\pi/\omega_m$ . Also, we assume the reference signal is a replica of the desired signal. Under these assumptions the array weights with the DPSK biphase modulated desired signal are the same as those produced with a CW signal. The effective bit error probability  $\bar{P}_e$  has been obtained by averaging the instantaneous bit error probability over one period of the interference modulation. The instantaneous bit error probability  $P_e(t')$  is related to the SINR by [12],

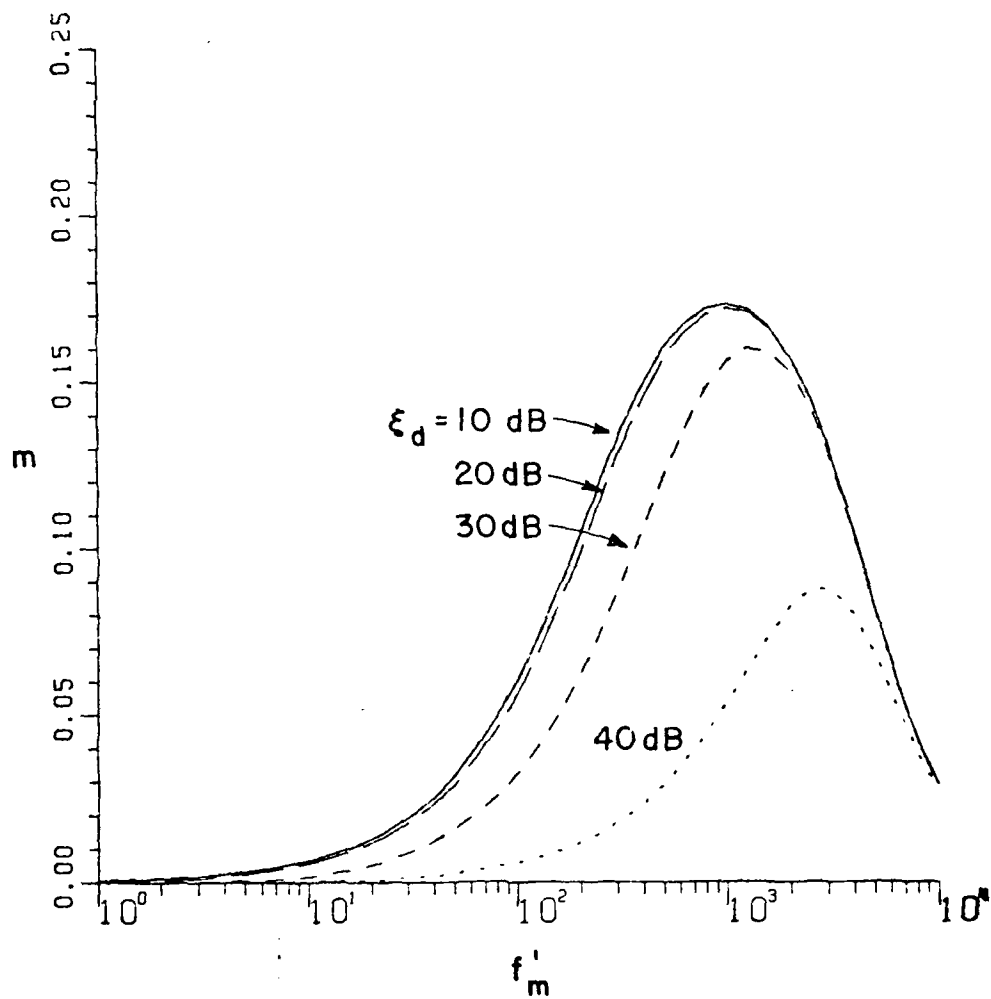


Figure 11.  $m$  versus  $f'_m$ .

$\theta_d=30^\circ$ ,  $\theta_i=45^\circ$ ,  $\xi_d=30$  dB,

$\beta=10^4$ ,  $f'_0=10^8$ .

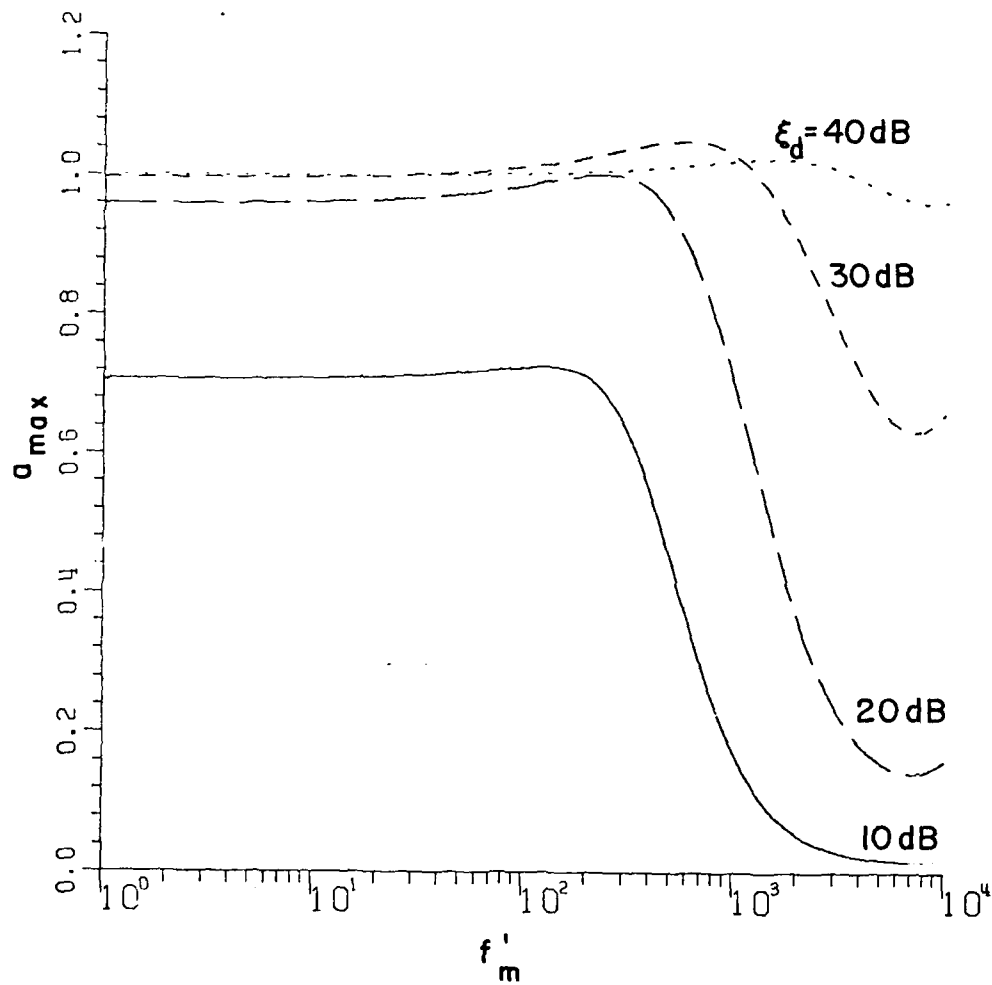


Figure 12.  $a_{\max}$  versus  $f'_m$ .

$\theta_d = 30^\circ$ ,  $\theta_i = 45^\circ$ ,  $\xi_d = 30\text{ dB}$ ,

$\beta = 10^4$ ,  $f'_0 = 10^8$ .

$$P_e(t') = \frac{1}{2} e^{-\text{SINR}(t')} \quad (73)$$

Figure 13 shows typical curves of  $\bar{P}_e$  as a function of  $f'_m$  for  $\theta_d=30^\circ$ ,  $\theta_i=45^\circ$ ,  $\xi_d=10$  dB,  $\xi_i=30$  dB,  $f'_0=10^8$  and for four values of  $\beta$  between  $2 \times 10^3$  and  $10^4$ . At low  $f'_m$ , where the interference bandwidth is too small to cause any degradation in the array performance,  $\bar{P}_e$  stays constant at a value that does not depend on  $\beta$ . This value of  $\bar{P}_e$  is determined simply by the input INR. As  $f'_m$  increases the interference bandwidth has more effect. At high  $f'_m$ ,  $\bar{P}_e$  approaches 0.5.

Figure 14 shows typical curves of  $\bar{P}_e$  versus  $f'_m$  for different values of  $\xi_i$  and for  $\theta_d=30^\circ$ ,  $\theta_i=45^\circ$ ,  $\xi_d=10$  dB,  $f'_0=10^8$  and  $\beta=10^4$ . These curves illustrate the dependence of  $\bar{P}_e$  on the interference power. At low  $f'_m$ , the interference has small bandwidth and  $\bar{P}_e$  depends slightly on  $\xi_i$ . This behavior is the same as with CW interference.

#### IV. CONCLUSIONS

We have developed a method for finding the periodic steady-state weights of an adaptive array receiving an interference signal with periodic angle modulation. We then used this method to study the behavior of a two-element array subjected to an interference signal with sinusoidal phase modulation. This interference causes the array weights to cycle sinusoidally with time, both in magnitude and phase. The modulated weights cause the desired signal to have envelope (but not phase) modulation at the array output.

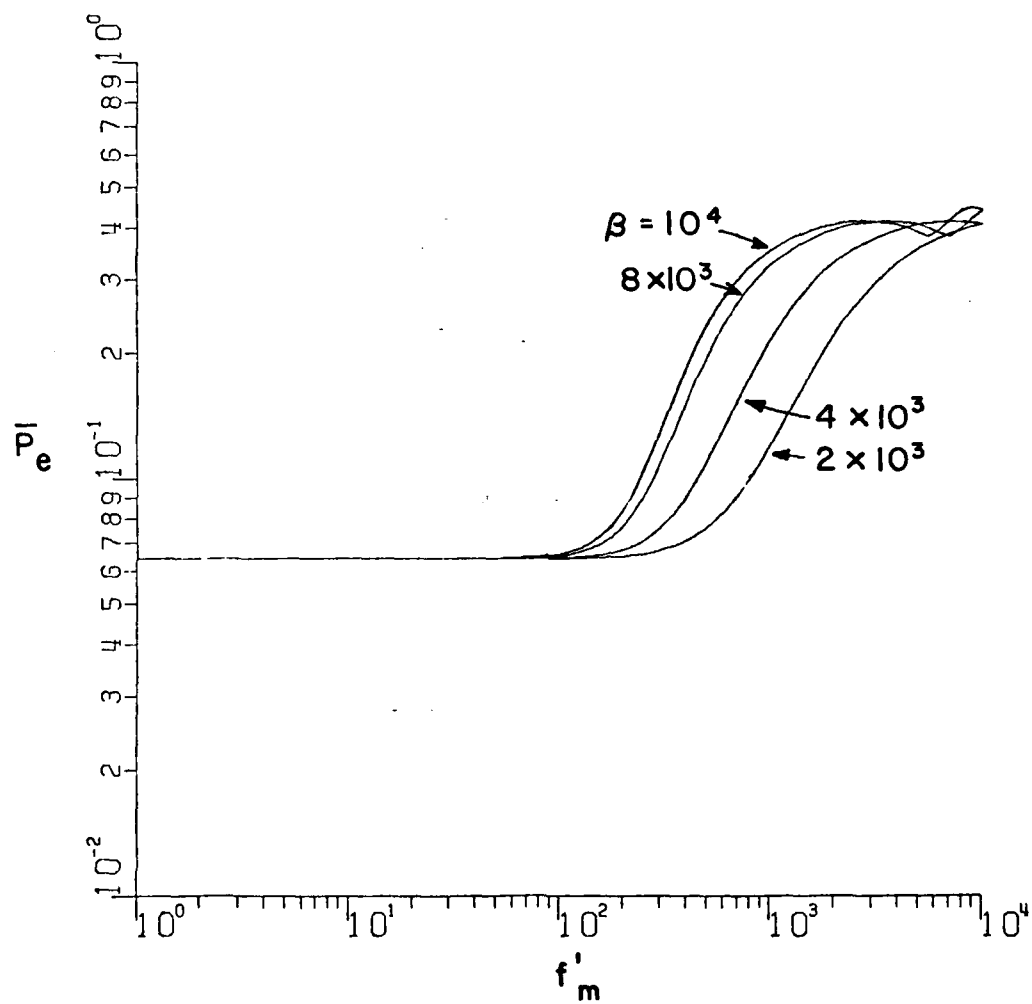


Figure 13. Bit error probability versus  $f'_m$ .

$\theta_d=30^\circ$ ,  $\theta_i=45^\circ$ ,  $\epsilon_d=10$  dB,

$\epsilon_i=30$  dB,  $f'_0=10^8$ .

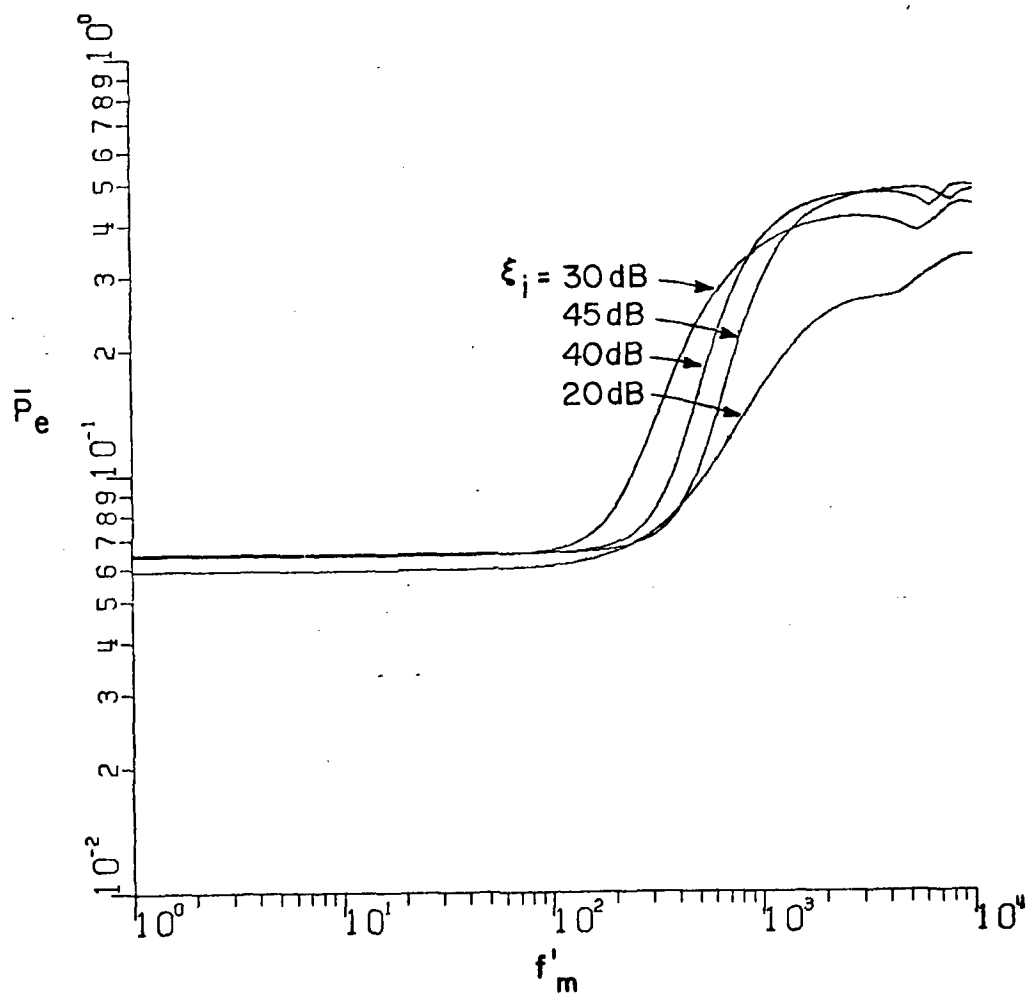


Figure 14. Bit error probability versus  $f'_m$ .

$\theta_d=30^\circ$ ,  $\theta_i=45^\circ$ ,  $\xi_d=10\text{ dB}$ ,

$\beta=10^4$ ,  $f'_0=10^8$ .

The envelope modulation is largest when the interference arrives close to the desired signal in space. The envelope modulation increases with the bandwidth of the input interference signal. Phase modulated interference also causes the array output SINR to vary with time. When the array is used in a digital communication system, such SINR variation increases the bit error probability.

## REFERENCES

- [1] B. Widrow, P.E. Mantey, L.J. Griffiths and B.B. Goode, "Adaptive Antenna Systems", *Proc. IEEE*, Vol. 55, p. 2143, December 1967.
- [2] R.T. Compton, Jr., "The Effect of a Pulsed Interference Signal on an Adaptive Array", *IEEE Trans. Aerospace and Electronic Systems*, Vol. AES-18, p. 297, May 1982.
- [3] A.S. Al-Ruwais and R.T. Compton, Jr., "Adaptive Array Behavior with Sinusoidal Envelope Modulated Interference", Report 713603-5, The Ohio State University ElectroScience Laboratory, Department of Electrical Engineering; prepared under Contract No. N00019-81-C-0093 for Naval Air Systems Command, March 1982.
- [4] A.S. Al-Ruwais and R.T. Compton, Jr., "Adaptive Array Behavior with Periodic Envelope Modulated Interference", Report 714505-1, The Ohio State University ElectroScience Laboratory, Department of Electrical Engineering; prepared under Contract No. N00019-82-C-0190 for Naval Air Systems Command, December 1982.
- [5] R.T. Compton, Jr., R.J. Huff, W.G. Swarner and A.A. Ksienski, "Adaptive Arrays for Communications Systems: An Overview of Research at The Ohio State University", *IEEE Trans. Antennas and Propagation*, Vol. AP-24, p. 599, September 1978.
- [6] R.T. Compton, Jr., "An Adaptive Array in a Spread Spectrum Communication System", *Proc. IEEE*, Vol. 66, p. 289, March 1978.
- [7] J.H. Winters, "Spread Spectrum in a Four-Phase Communication System Employing Adaptive Antennas", *IEEE Trans. on Communications*, Vol. COM-30, p. 929, May 1982.
- [8] H. D'Angelo, Linear Time-Varying Systems: Analysis and Synthesis, Allyn and Bacon, Boston, 1970.
- [9] D.M. Young and R.T. Gregory, A Survey of Numerical Mathematics, Addison-Wesley Publishing Co., Reading, Massachusetts, 1972.
- [10] P.M. Morse and H. Feshbach, Methods of Theoretical Physics, McGraw-Hill Book Co., New York, 1953; p. 620.



- [11] R.E. Ziemer and W.H. Tranter, Principles of Communications, Houghton-Mifflin, Boston, 1976.
- [12] W.C. Lindsey and M.K. Simon, Telecommunication Systems Engineering, Prentice-Hall, Englewood Cliffs, New Jersey, 1973.

END

DATE  
FILMED

10-83

DTI